Springer

Chinese Society of Pavement Engineering

International Journal of
Pavement Research and Technology

Journal homepage: www.springer.com/42947

Sensor-based pavement diagnostic using acoustic signature for moduli estimation

S. Cafiso[a]*, A. Di Graziano[a], R. Fedele[b], V. Marchetta[a], F. Praticò[b]

[a] *Department of Civil Engineering and Architecture, University of Catania, Via Santa Sofia 64, I-95125 Catania, Italy*
[b] *Department of Information Engineering, Infrastructure and Sustainable Energy, University Mediterranean of Reggio Calabria, Italy*

Received 19 November 2020; received in revised form 20 November 2020; accepted 23 November 2020

Abstract

The diffusion of smart infrastructures for smart cities provides new opportunities for the improvement of both road infrastructure monitoring and maintenance management.

Often pavement management is based on the periodic assessment of the elastic modulus of the bound layers (i.e., asphalt concrete layers) by means of traditional systems, such as Ground Penetrating Radar (GPR) and Falling Weight Deflectometer (FWD). Even if these methods are reliable, well-known, and widespread, they are quite complex, expensive, and are not able to provide updated information about the evolving structural health condition of the road pavement. Hence, more advanced, effective, and economical monitoring systems can be used to solve the problems mentioned above.

Consequently, the main objective of the study presented in this paper is to present and apply an innovative solution that can be used to make smarter the road pavement monitoring. In more detail, an innovative Non-Destructive Test (NDT)-based sensing unit was used to gather the vibro-acoustic signatures of road pavements with different deterioration levels (e.g. with and without fatigue cracks) of an urban road. Meaningful features were extracted from the aforementioned acoustic signature and the correlation with the elastic modulus defined using GPR and FWD data was investigated.

Results show that some of the features have a good correlation with the elastic moduli of the road section under investigation. Consequently, the innovative solution could be used to evaluate the variability of elastic modulus of the asphalt concrete layers, and to monitor with continuity the deterioration of road pavements under the traffic loads.

Keywords: In-situ measurements; Pavement condition; Elastic modulus; FWD; NDT smart sensors

1. Introduction

Smart roads will provide new opportunities for sustainable, efficient, safe and resilient transportation infrastructures. By improving both monitoring and maintenance processes (e.g., moving from failure-based to a condition- or prediction-based approach exploiting systems able to carry out continuous monitoring), pavement needs can be timely identified and this leads to reduce total costs and extend service life [1-3]. Reliability and effectiveness of traditional approaches both in-lab analysis of pavement samples as cores or slabs and NDT on-site investigations (e.g. Ground Penetrating Radar, GPR, Falling Weight Deflectometer, FWD, and Light Weight Deflectometer, LWD) are well-known. Nevertheless, they lack in cost (i.e., are based on expensive devices or destructive tests), in safety (i.e., implying the closure of the road section under test, negatively affecting traffic and road safety) and in continuity (i.e., are based on stand-alone devices). Based on the limitations listed above, the concept of Intelligent Transportation Systems [4] emerged and a multitude of solutions have been proposed. Usually, sensor-based devices and technologies are used as in-vehicle equipment for automatic and continuous assessment, or are embedded or positioned on the pavement to form a network.

More extensively, in terms of classification and analysis of monitoring, it is possible to highlights the following different solutions for road pavements:

1. embedded [5-7] and non-embedded sensor-based systems [8,9];
2. mobile [10-12] and stationary systems [13-14];
3. wireless [15,16], wired [17,18] and self-powered systems [19,20];
4. traditional [21,22] and smart data management [23-25];

Despite the promising advantages of the sensor-based solutions, and the growing need of infrastructures in the Internet of Things (IoT) world, it must be underlined that these solutions are sometimes in an early stage of investigation, and that there is a lack of applications in real contexts. Based on the above, the main objective of the presented study is to validate the results of an innovative road pavement monitoring solution with data derived

* Corresponding author
E-mail address: dcafiso@unict.it (S. Cafiso).
Peer review under responsibility of Chinese Society of Pavement Engineering.

ISSN: 1997-1400 DOI: https://doi.org/10.1007/s42947-020-6007-4
Chinese Society of Pavement Engineering. Production and hosting by Springer Nature

using traditional methods (i.e., GPR, FWD). In more detail, (1) different sections of the same road pavement with different damage levels were selected and characterized in terms of thickness using a GPR; (2) dynamic loads of different intensity were applied and deflections recorded with the FWD while (3) an innovative NDT solution was used to gather the vibro-acoustic signature of road sections during the load test; finally, (4) elastic moduli and innovative acoustic parameters (features) were extracted and analyzed in order to investigate the existence of a correlation between traditional and innovative pavement parameters.

The paper is so organized: the introduction is followed by a brief description of the methodological approach associated with each equipment used in the study, with more detail to the new vibro-acoustic sensor. The third section defines the experiment in the road where the test was carried out. The fourth section provides a description and discussion of data analysis and statistical correlation between traditional parameters and acoustic features. Finally, conclusions resume main results and focus on gaps and possible directions that future research could follow to allow the use of the proposed sensor for pavement health condition monitoring.

2. Methodological approach

2.1. Ground Penetration Radar (GPR)

The ground penetrating radar is a geophysical radar system that can provide a fast, non-destructive measurement technique for evaluating asphalt layer thickness and presence of infrastructural interferences within the pavement [26].

Since urban pavements present thin layers, it is often challenging to differentiate the reflection from the top and bottom of the layer. Antennas with a centre frequency of 2000 MHz can provide a sufficient resolution to measure a minimum layer thickness less than 2.5 cm (1 in.) with an accuracy of 0.25 cm (0.1 in.) (ASTM D4748) [27]. Moreover, when GPR approaches above a pipe, a cable duct or a manhole, the two-way travel time versus travel distance has a parabolic shape [28], so it is possible to highlight the presence of these types of interferences. The GPR used in the present study uses two antennas with 600 MHz and 2000 MHz frequencies to estimated layer thickness. The K2_FW® acquisition software [29] is used to manage the phases of radar acquisition and to review the data acquired directly in the field to select test sites without underground interferences.

2.2. Falling Weight Deflectometer (FWD)

The FWD is used for non-destructive field tests, which is designed to simulate the load conditions of a moving heavy vehicle and estimates the pavement's response by measuring the deflection basin with several sensors. The device allows a variable weight from 50 to 400 kg to be dropped from a variable height. The conventional FWD is able to apply loads in the range of 7÷140 kN, even if the standard load used for structural pavement analysis is usually 30÷50 kN over a circular load plate. The generated duration of the half sine pulse is typically 30 ms, corresponding to the loading time produced by a truck moving at 40 km/h. The FWD used in the present study is equipped with a loading plate of 300 mm diameter, 9 geophones positioned in the direction of the road, a load of 250 kg and 4 standard drop heights able to produce loads in the range 37-125 kN [30].

2.3. Vibro-acoustic sensors

The innovative solution mentioned above consists of a system and a method (Fig. 1) designed bearing in mind concepts such as innovation, sustainability, efficiency, and intelligence. The proposed solution aims at monitoring the Structural Health Status (SHS) of road pavements using the vibro-acoustic signature of the road gathered using a sensor network [1,31-33].

In more detail (Fig. 1): 1) The proposed monitoring method considers the road pavement as an "acoustic filter" with a given SHS. 2) The SHS depends on the presence of damages (e.g. cracks), which are usually produced by the traffic, and are generated inside the road (i.e., they may be hidden or not, usually localized under the wheel paths between bound and unbound layers). 3) The aforementioned method aims at detecting the variation of the SHS of a road pavement due to the occurrence or the propagation of also hidden damages (i.e., before they propagate to the road surface), which modify the "acoustic filter". 4) A network of sensing units is attached (non-destructive test, NDT, or non-destructive evaluation, NDE) on several sections of the road to monitor. 5) Seismic waves (ground-borne sounds and vibrations) are produced by different sources (e.g., vehicles - uncontrolled loads during the continuous monitoring - or deflectometers - controlled loads during a periodic assessment -), and propagate into the road layers. 6) The vibro-acoustic signatures, i.e., the acoustic responses of the road pavement sections to the given loads are recorded. In more detail, the variation of the air pressure inside each sensing unit (which consists of a microphone contained in an air-borne noise insulating coating) are detected and recorded. 7) The recorded signals are analysed in order to detect the worsening of the SHS of the road pavement (acoustic filter modification/deterioration). In the analyses, the variation of meaningful parameters (herein called features), extracted from the recorded signals, is used to represent the variation of the SHS of the monitored road in a simple and effective way.

In this study, a system consisting of a single sensing unit was used. In more detail, the system consists of the following devices: 1) Omnidirectional pre-polarized microphone "Audix TM1" (frequency response: 20-25 kHz ± 2 dB, sensitivity: 6 mV/Pa at 1 kHz, dynamic range: 112 dB), acoustically isolated using a plastic box filled with insulating material and modelling clay (used also to attach the box to the road). 2) External sound card "Roland quad-capture UA-55". 3) Recorder/Analyzer: ASUS ZenBook (model: UX433F, Intel® Core™ i7-8565U, RAM: 16 GB, 64bit x64) running MATLAB codes that allow recording acoustic signals with a sampling frequency of 192 KHz.

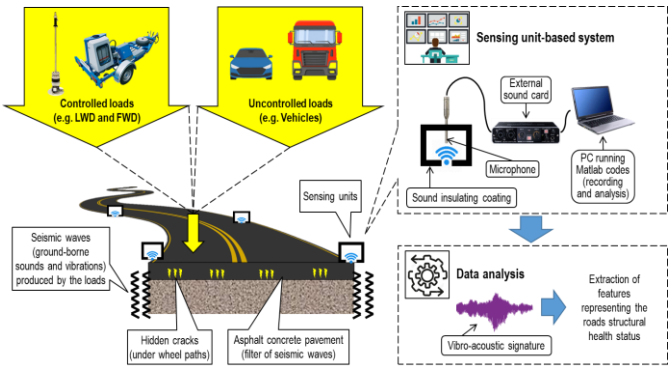

Fig 1. Schematic representation of the innovative monitoring solution.

It is important to underline that the sensing system used in this study is one of the possible systems that can be used as a receiver able to apply the method above. This is going to be improved to obtain a self-powered wireless sensor network in order to address some of the objectives of the ongoing Italian project USR342-PRIN 2017-2022.

3. Road trial test

In order to identify the sites to be investigated during the road test, the Ground Penetrating Radar was used. About 300 meters long urban road in Catania (Italy) were covered in both directions, for a total of about 600 meters.

The thickness of the asphalt layer was analysed along the entire path with a step of 1 meter and the presence of any underground services was identified. Only the areas without underground facilities and with asphalt layer thickness more than 15 cm were taken into account. Through a visual inspection, four sections were selected, two without surface cracking and two with alligator cracks (Fig. 2). In each of the identified pavement areas, the test was carried out by loading the pavement with the FWD following the schema reported in the right part of Fig. 3.

In particular, once the vibro-acoustic sensor has been positioned on the pavement area under consideration, the load tests were carried out with the FWD plate in line with the microphone at a distance of 1.5 meters. Then, for the sections 1 and 2, other two load tests were carried out moving the plate one meter back and the one meter forward along the direction of travel.

During the tests carried out with the FWD, the mass was dropped with two series of 4 different heights in order to obtain 4 loads of about 40-56-84 and 120 kN. Therefore, for each load and position the FWD test was performed 4 times (i.e. 2 drops for each of the two series).

4. Data analysis

4.1. Load deflection data

As a preliminary part of the data analysis, the collected 128 FWD load/deflection data were verified, in order to discard the measures that did not respect the following conditions [34]:

1. Load variation consistency. This refers to the conditions where the drop load varies by more than 0.18 kN (40.5 lbf) plus 2% of the average load.
2. Deflection variation consistency. This refers to deviations from the same drop height that vary by more than 2 μm (0.08 mils) plus 1% of the mean deflection.

104 FWD tests were selected for the moduli back-calculation with the ELMOD® software [35]. The structure of the pavement was defined as a double layer composed of a subgrade and an asphalt surface layer with thickness equal to 150 mm in the first section, 130 mm in the second, 181 mm in the third and 175 mm in the fourth, as identified by the GPR output. A Finite Element Method (FEM) analysis was carried out to calculate the moduli of the asphalt layer taking into account the non-linear subgrade behaviour. Fig. 4 shows the average moduli in each drops sequence for the different sections and plate positions (Fig. 3).

4.2. Acoustic signature data

Fig. 5 shows two examples of vibro-acoustic signature of the road pavement under investigation. Signals were recorded using

Fig. 2. Selection of pavements in different conditions.

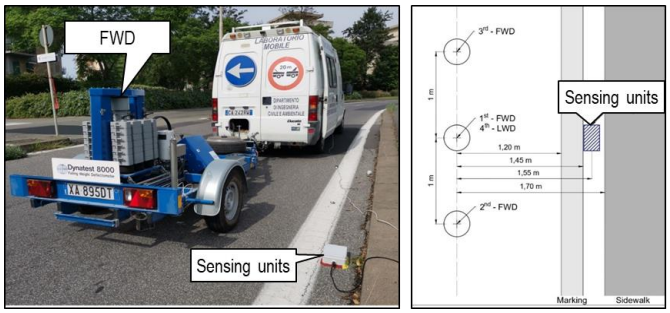

Fig 3. Set of equipment composed by FWD and acoustic sensor.

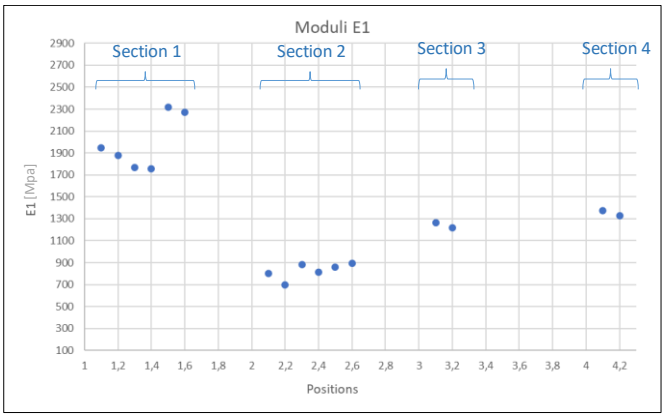

Fig. 4. Average Moduli E_1 of the asphalt layer at different sections.

the aforementioned NDT sensing unit, and are presented in two different domains of analysis, i.e., time (amplitude *versus* time, cf. 5a and 5b) and frequency (Power Spectral Density, PSD, *versus* frequency in 1/3 octave bands, 5c and 5d). Fig. 5 shows an example of the vibro-acoustic signatures of the sections 1.2 and 2.2, loaded at 38 kN. Note that sections 1.2 and 2.2 are located in the position "2nd-FWD" in Fig. 3.

The signals in Fig. 5 were selected aiming at showing how the signature of the same pavement varies if different sections (i.e., section 1.1 and 2.2) are considered. It is important to underline that the FWD produces impulse loads generated by a mass that falls on buffers which allow the mass to rebound several times until all the energy is dissipated. Hence, the impulse responses of the road pavement to the FWD loads consist of a "first rebound" followed by other rebounds. Note that in this study only the "first rebound" is used for the calculation of the elastic modulus, and, for this reason, this part of each signal was used as the vibro-acoustic signature of the road. Note that the main difference among the "all rebounds" spectra and the "first rebounds" spectra is that the PSD amplitude of the second ones is slightly greater than that of the first ones. Based on Figs. 5(a) and 5(b) 1) The amplitude of the signal

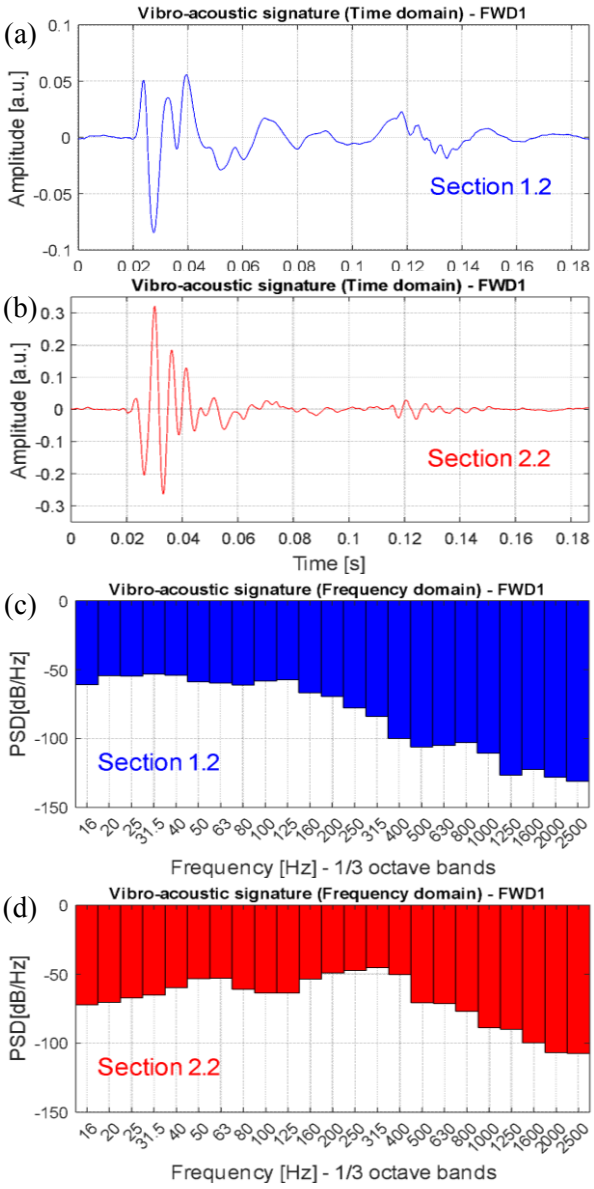

Fig. 5. Vibro-acoustic signatures: (a) section 1.2 (time domain), (b) section 2.2 (time domain), (c) section 1.2 (frequency domain), and (d) section 2.2 (frequency domain).

related to section 2.2 is three times greater than the one of section 1.2. 2) The damping of section 2.2-related signals is greater than the one of section 1.2-related signals.

The differences in terms of amplitudes could be due to 1) The elastic moduli of the bound layers (on average, section 1.2 modulus is about 1200 MPa greater than that of section 2.2). 2) The elastic moduli of the unbound layers (on average, section 1.2 modulus is about 70 MPa greater than that of section 2.2). 3) The thickness of the bound layer (on average, section 1.2 thickness is about 2 cm greater than that of section 2.2).

The differences in terms of signal length could be due to the energy dissipation caused by different structural health conditions of the sections under test, which, in turn, could be related to elastic moduli (especially for bound layers) and to the extracted features.

Based on the previous studies [31,36] and on the shape of the vibro-acoustic signatures of the sections under investigation (cf. Fig. 5), five features were extracted. In more detail, the following two features were identified and extracted in the time domain (see Fig. 6(a)):

1. *Feature 1 (F1)*, i.e., the difference between the absolute maximum P and the absolute minimum N of the vibro-acoustic signature amplitudes (arbitrary unit, a.u.);
2. *Feature 2 (F2)*, i.e., the time delay between P and N (milliseconds); while, the following ones were recognized and used in the frequency domain (see Fig. 6(b)):
3. *Feature 3 (F3)*, i.e., the spectral centroid of the spectrum (see the star in Fig. 6(b)) in the frequency range 16÷2500 Hz, which can be defined as the "centre of mass" of a spectrum [37] (Hz);
4. *Feature 4 (F4)*, i.e., the slope of the linear regression model applied on the spectrum (PSD vs. frequency) in 16÷2500 Hz (dBW);
5. *Feature 5 (F5)*, i.e. the maximum of the spectrum in 16÷2500 Hz (dBW/Hz).

Finally, Table 1 provides an overview of the features extracted for each section of the road pavement under test.

4.3. Correlations

88 out of the 104 FWD load tests were selected to analyse the capability of the acoustic features to capture the variability in the pavement elastic modulus. Sixteen tests were excluded because of signal saturations occurred during the measurements in section 2.

The summary statistics of the measures derived from the collected data (Table 2) show a wide range of moduli E_1 with standardized skewness and kurtosis in the range -2 to +2 indicating a shape in accordance with a normal distribution. In the test sections we can assume homogeneous asphalt concrete mixtures.

As first attempt to analyse the existence of correlation between actual elastic moduli determined by the load-deflection data with the different features derived from the acoustic signatures of the pavement sections, we analysed the results of the correlation

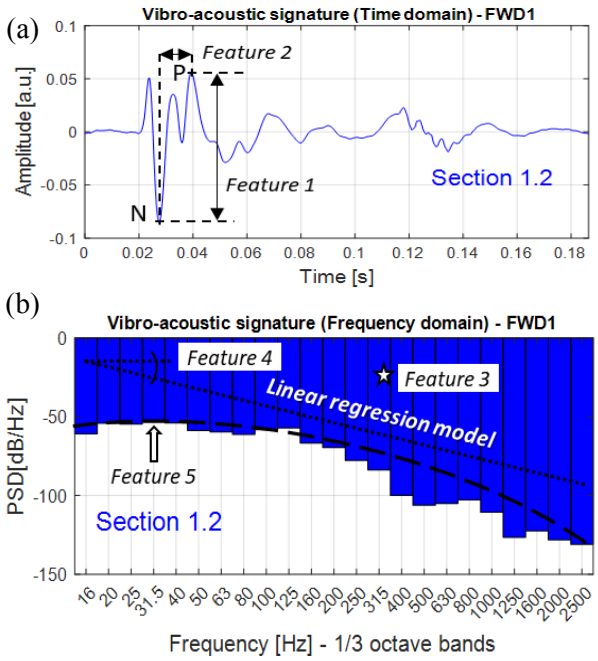

Fig. 6. Graphical representation of the features extracted in the (a) time and the (b) frequency domains of analysis.

matrix reported in Table 3. All the features showed a significant correlation with E_1, with p-values less than 0.05. The higher correlation coefficients are for F2, F3, F4 and F5. These features are also significantly correlated to each other.

Pearson correlation coefficient is traditionally used in a cross-sectional study, because it is not theoretically appropriate in longitudinal studies with repeated-measure as it ignores the correlation of the outcomes within the same subject [38,39]. Moreover, the Pearson correlation statistic indicates the strength of a linear relationship between two variables, but it does not completely characterize the shape of the relationship.

In the present study, tests were conducted with different loads applied in the same plate position. Therefore, observations may be interdependent, because different load tests nested in the same plate position are more likely to function in the same manner than tests that refer to different sections. If the observed outcomes are not independent, the effective sample size decreases, and thus, failure to account for the intra-cluster correlation in conventional analyses negatively affects the precision of the estimates. A generalized estimating equation (GEE) is a method based on quasi-likelihood estimation for longitudinal marginal models that allows a valid inference by implicitly taking into account the correlation to obtain the correct standard errors of the regression coefficient estimates [40]. Therefore, a GEE study was carried out in order to account for the repeated measures and to define a more refined estimation of the correlation between the modulus and the acoustic signature of the pavement.

In the GEE modelling, the total sample was composed of 24 tests (i.e., one for each load value), clustered in 8 plate positions with the number of load repetitions ranging from 1 to 4 (Table 4).

Different linear regression models were evaluated for each feature applying variable transformations to improve the goodness of fit. We used the Quasi-likelihood under Independence model Criterion (QIC) to choose between different variable transformations. The models that obtain smaller QIC are "better" according to this criterion.

Moreover, in order to show a more usual goodness-of-fit measure like the R-squared in ordinary least squares regression,

Table 1
Feature statistics.

Feature	Section	Statistics			
		Max	Min	Average	St.dev.
F1 [a.u]	1	0.532	0.078	0.277	0.143
	2	0.922	0.274	0.587	0.201
	3	0.578	0.317	0.422	0.090
	4	0.527	0.179	0.320	0.124
F2 [ms]	1	12.042	3.344	7.599	2.906
	2	3.516	2.969	3.249	0.189
	3	3.115	2.839	3.038	0.099
	4	10.552	4.563	6.940	2.654
F3 [Hz]	1	724.000	641.000	679.833	18.788
	2	689.000	620.000	651.929	22.705
	3	694.000	624.000	654.700	22.961
	4	706.000	627.000	669.063	23.258
F4 (%)	1	-2.700	-4.099	-3.292	0.351
[dbW]	2	-2.055	-3.407	-2.648	0.431
	3	-2.310	-3.491	-2.858	0.463
	4	-2.259	-3.711	-3.001	0.440
F5	1	80.000	31.500	56.104	23.954
[dbW/Hz]	2	315.000	25.000	202.857	93.746
	3	315.000	160.000	241.500	74.366
	4	160.000	20.000	54.344	34.641

Symbols. St. dev. = Standard deviation; F1= Feature 1; a.u. = arbitrary unit; F2 = Feature 2; ms = milliseconds; F3 = Feature 3; Hz = Hertz; F4 = Feature 4; dBW = decibel Watt; F5 = Feature 5z.

Table 2
Summary statistics of the measures.

	E_1 [Mpa]	F1 [a.u.]	F2 [ms]	F3 [Hz]	F4 [dBW]	F5 [dBW/H]	Load [kN]	H_1[mm]
Count	**88**	**88**	**88**	**88**	**88**	**88**	88	88
Average	1599.62	0.35072	6.26876	670.58	-3.08714	100.199	71.4659	154.8
Stnd. deviation	524.57	0.18526	3.11279	23.8832	0.468474	89.6515	30.9452	16.29
c. of variation	32.79%	52.82%	49.65%	3.56%	-15.17%	89.47%	43.30%	10.52%
Minimum	570.5	0.07824	2.83854	620.0	-4.09893	20.0	37.0	130.0
Maximum	2776.6	0.9222	12.0417	724.0	-2.05492	315.0	125.0	181.0
Range	2206.1	0.8440	9.20313	104.0	2.04401	295.0	88.0	51.0
Stnd. skewness	0.320	3.1002	2.07351	-0.77913	0.573674	5.78352	2.27127	0.904
Stnd. kurtosis	-1.316	1.0089	-2.4235	-0.67962	-0.65253	2.25939	-1.9121	-1.714

Table 3
Correlation coefficients and p-values *(in italic)*.

	F1	F2	F3	F4	F5
E_1	-0.2663	0.5628	0.5510	-0.4721	-0.5706
	(0.0122)	*(0.0000)*	*(0.0000)*	*(0.0000)*	*(0.0000)*
F1		-0.0622	0.0881	0.2056	0.3666
		(0.5651)	*(0.4144)*	*(0.0546)*	*(0.0004)*
F2			0.5394	-0.3855	-0.5147
			(0.0000)	*(0.0002)*	*(0.0000)*
F3				-0.8945	-0.6253
				(0.0000)	*(0.0000)*
F4					0.6636
					(0.0000)

Table 4
Summary data for the GEE model.

Data Summary			
Number of Levels	Subject Effect	Position	8
	Within-Subject Effect	Load	4
Number of Subjects			8
Number of Measurements per Subject	Minimum		1
	Maximum		4
Correlation Matrix Dimension			4

Table 5
Results from the GEE models (All the model are in the form: $E_1=A + B \cdot X$).

Variable (X)	P-value	QIC	Pseudo R^2	MAPE	Intercept (A)	Coefficient (B)
F1	0.011	5961702	14%	30.3%	1928.973	-1041.637
Exp(F1)	0.002	5825225	16%	29.4%	2589.051	-708.197
F2	0.000	4232128	39%	25.1%	867.753	112.132
1/F2	0.000	3881310	44%	25.1%	2351.882	-3854.346
F3	0.000	3756567	46%	26.2%	-11487.748	19.456
F4	0.000	3339880	52%	20.7%	-2333.805	-1264.833
F5	0.000	3313262	52%	23.3%	2072.377	-4.743
Sqrt(F5)	0.000	3251594	53%	22.8%	2620.321	-108.485
Intercept	0.000	6941307	0%		1540.938	

the Pseudo R^2 is computed, assuming that the ratio of the log likelihoods of the model (LL_{model}) to the one of the intercept model ($LL_{intercpet}$) suggests the level of improvement over the intercept model offered by the full model [41]. McFadden's Pseudo Rsquare is defined as $R^2 = 1-(LL_{model}/LL_{intercpet})$. Results from the GEE models are reported in Table 5.

Based on the data reported in Table 5, the following results can be highlighted:

1. The p-values of the features are less than 0.05 in all the regression models;
2. F4 and F5 (i.e., Sqrt(F5)) resulted the best fitting parameters with the smallest QIC, the highest R^2 and lowest mean absolute percentage error (MAPE);
3. F3 and F2 (i.e., 1/F2) showed intermediate results;
4. F1, even in the best variable transformation (i.e., Exp(F1)), performed worse than the other features.

4.4. *Discussion*

While, the GEE statistics shows the goodness of fit of the different features, this section refers to the shape of the regression curve between moduli and features derived using the statistical analysis reported in the previous section (cf. Table 5). In more detail, in Fig. 7 different indicators show the data sample in the four sections and dashed black lines show the best fit regression models derived for each feature.

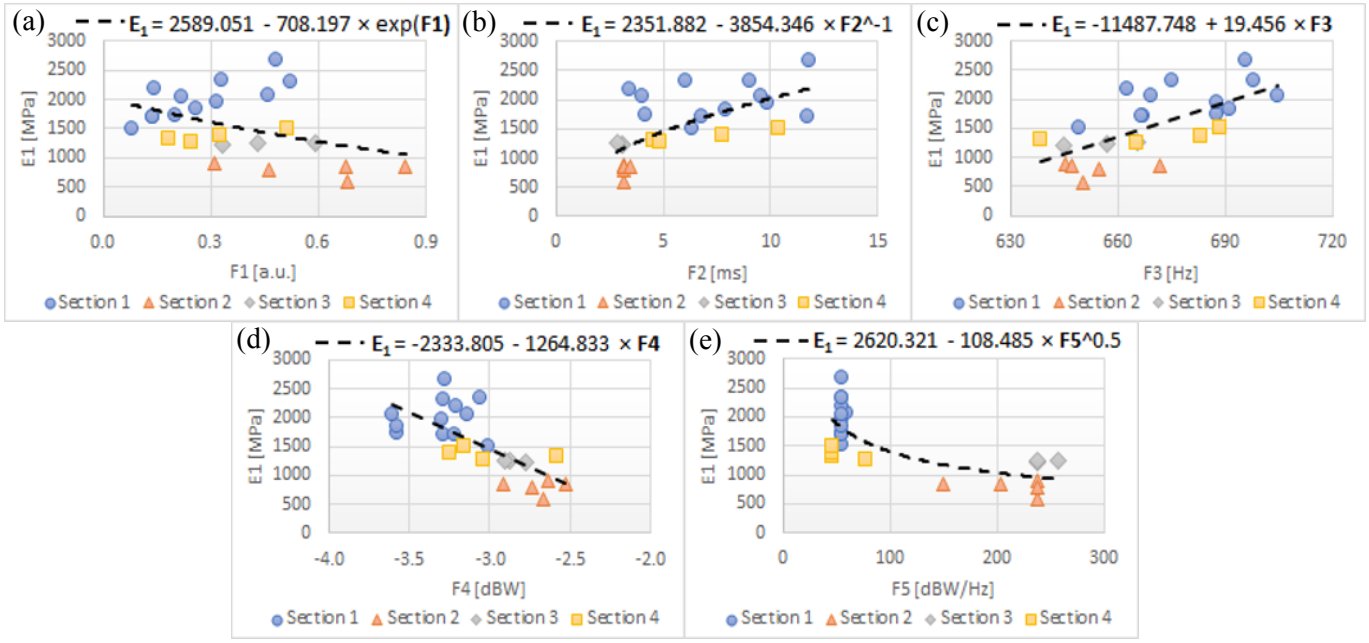

Fig. 7. FWD Elastic Moduli (E_1) vs. vibro-acoustic features and best fit regression curves: (a) F1, (b) F2, (c) F3, (d) F4, and (e) F5.

Note that the elastic modulus varies in the range interval 500÷3000 MPa and lower moduli in sections 2 and 3 can be associated with the existence of damages (surface and/or internal) in the asphalt concrete layers. Based on Fig. 7, it is possible to observe that:

1. Sections 1 and 4 (which did not show surface damages) has the highest moduli, while sections 2 and 3 (where surface cracks were observed and where internal damages could be present) have the lowest moduli.
2. Furthermore, several plots seem to suggest that there are two main clusters, i.e., cluster H (yellow squares & blue circles, i.e., sections 4 & 1) and cluster L (orange triangles & grey rhombuses, i.e., sections 2 & 3). The distance between these clusters is sometimes negligible (features 1, 3, and 4) but seems higher when considering the features number 2 and 5.
3. Based on the above, features 2 and 5 seem to be able to better detect the presence of asphalt layer cracks (sections 2 & 3) and to better distinguish the cracked (2 & 3) from the uncracked (1 & 4) sections.
4. As mentioned above, surface cracks mainly refer to sections 2 and 3 and the features number 2 and 5 seem to detect this occurrence, but while higher crack-related damages refer to higher values of the feature number 5, they yield lower values of the feature number 2.

Overall, even if several features appear to better interpret the structural health conditions, it is possible to observe that higher densities of cracks relate to higher values in terms of the features 1 and 4 (respectively, signal amplitude and PSD slope) and to lower values in terms of features 2, 3, and 5 (respectively, time lag, centroid and slope).

5. Conclusions

This study examined the possibility to use the features extracted from the vibro-acoustic signature of a road pavement to evaluate the structural health status and the elastic moduli of a road pavement. An innovative approach and NDT sensing device were used to gather the aforementioned signatures in terms of response to traffic loads simulated by a FWD. This device was also used to estimate the elastic modulus of pavement layers.

Results show that some features have a good correlation with the elastic modulus and that both signals over time and spectra can offer insights in terms of moduli and structural health conditions. Consequently, these features could be used to recognize the worsening of the structural status of pavement layers associated with a reduction of the elastic modulus and propagation of cracks.

The main challenge of the method proposed in this study is the selection of the features that should be able to recognize changes of elastic moduli and structural conditions. Experiments and data provided valuable information about the higher or lower dependence of acoustic features on loads and other boundary conditions. These observations could be crucial in terms of method potential and application.

Future work will include the extension of the pavement sample and the investigation about the relationship between features and load intensity and frequency.

Acknowledgement

This work has been partially financed by the PRIN 2017-2022 within the ongoing project USR342, by the University of Catania within the project TIMUC (PIACERI) and by the European Commission social fund and the Calabria Region (PAC Calabria 2014-2020).

Conflicts of interest

There is no conflicts of interest

Reference

[1] R. Fedele, Smart road infrastructures through vibro-acoustic signature analyses, Smart Innov. Syst. Technol. 178 (2020) 1481–1490.
[2] J.B. Odoki, A. Di Graziano, R. Akena, A multi-criteria methodology for optimising road investments, Proc. Inst. Civ. Eng. Transp. 168 (1) (2015) 34–47.
[3] F.G. Praticò, Roads and Loudness: A More Comprehensive Approach, Road Mater. Pavement Des. 2 (4) (2001) 359–377. https://doi.org/10.1080/14680629.2001.9689908
[4] J. Guerrero-Ibáñez, S. Zeadally, J. Contreras-Castillo, 2018. Sensor technologies for intelligent transportation systems, Sensors 18 (4) (2018) 1212.
[5] N. Bahrani, J. Blanc, P. Hornych, F. Menant, Alternate method of pavement assessment using geophones and accelerometers for measuring the pavement response, Infras. 5 (3) (2020) 25 https://doi.org/10.3390/infrastructures5030025
[6] H. Hasni, A.H. Alavi, P. Jiao, N. Lajnef, K. Chatti, K. Aono, S. Chakrabarty, A new approach for damage detection in asphalt concrete pavements using battery-free wireless sensors with non-constant injection rates, Meas. J. Inter. Meas. Confed. 110 (2017) 217–229.
[7] M. Manosalvas-Paredes, R. Roberts, M. Barriera, K. Mantalovas, Towards more sustainable pavement management practices using embedded sensor technologies, Infras. 5 (1) (2020) 4 https://doi.org/10.3390/infrastructures5010004
[8] M. Iodice, J.M. Muggleton, E. Rustighi, The in-situ evaluation of surface-breaking cracks in asphalt using a wave decomposition method. Nondestruct. Test. Eval. (2020) https://doi.org/10.1080/10589759.2020.1764553
[9] F.G. Praticò, R. Fedele, D. Vizzari, Significance and reliability of absorption spectra of quiet pavements, Constr. Build. Mater. 140 (2017) 274–281 https://doi.org/10.1016/j.conbuildmat.2017.02.130
[10] F. Bianco, L. Fredianelli, F. Lo Castro, P. Gagliardi, F. Fidecaro, G. Licitra, Stabilization of a p-u sensor mounted

on a vehicle for measuring the acoustic impedance of road surfaces, Sensors 20 (5) (2020) 1239.
[11] S. Cafiso, A. Di Graziano, D.G. Goulias, C. D'Agostino, Distress and profile data analysis for condition assessment in pavement management systems, Inter. J. Pavement Res. Technol. 12 (5) (2019) 527–536. https://doi.org/10.1007/s42947-019-0063-7
[12] C.W. Yi, Y.T. Chuang, C.S. Nian, Toward Crowdsourcing-Based Road Pavement Monitoring by Mobile Sensing Technologies, IEEE Trans. Intell. Transp. Syst., Piscataway, NJ, USA, 16 (4) (2015) 1905–1917
[13] F.M. Fernandes, J.C. Pais, Laboratory observation of cracks in road pavements with GPR, Constr. Build. Mater. 154 (2017) 1130-1138
[14] R. Grace, Sensors to support the IoT for infrastructure monitoring: technology and applications for smart transport/smart buildings, MEPTEC-IoT, San Jose, CA, USA, 2015.
[15] H. Ceylan, M.B. Bayrak, K. Gopalakrishnan, Neural networks applications in pavement engineering: A recent survey, Inter. J. Pavement Res. Technol. 7 (6) (2014) 434-444.
[16] A. Di Graziano, V. Marchetta, S. Cafiso, Structural health monitoring of asphalt pavements using smart sensor networks: A comprehensive review, J. Traffic Transp. Eng. (English Ed) 7 (5) (2020) 639-651.
[17] T. Iuele, F.G. Praticò, R. Vaiana, Fine aggregate properties vs asphalt mechanical behavior: An experimental investigation, in: Pavement and Asset Management, Proc. World Conference on Pavement and Asset Management, WCPAM, Baveno, Italy, 2017.
[18] Y. Yu, X. Zhao, Y. Shi, J. Ou, Design of a real-time overload monitoring system for bridges and roads based on structural response. Meas, J. Inter. Meas. Confed. 46 (1) (2013) 345–352. https://doi.org/10.1016/j.measurement.2012.07.006.
[19] R. Fedele, M. Merenda, F.G. Praticò, R. Carotenuto, F.G. Della Corte, Energy harvesting for IoT road monitoring systems, Instrum. Mes. Metrol. 18 (4) (2018) 605–623.
[20] H. Hasni, A.H. Alavi, K. Chatti, N. Lajnef, A self-powered surface sensing approach for detection of bottom-up cracking in asphalt concrete pavements: Theoretical/numerical modeling. Constr. Build. Mater. 144 (2017) 728–746.
[21] D. Mounier, H. Di Benedetto, C. Sauzéat, Determination of bituminous mixtures linear properties using ultrasonic wave propagation. Constr. Build. Mater. 36 (2012) 638–647.
[22] Y.O. Ouma, M. Hahn, Pothole detection on asphalt pavements from 2D-colour pothole images using fuzzy c-means clustering and morphological reconstruction, Autom. Constr. 83 (2017) 196–211 https://doi.org/10.1016/j.autcon.2017.08.017
[23] H. Ceylan, K. Gopalakrishnan, S. Kim, P.C. Taylor, M. Prokudin, A.F. Buss, Highway infrastructure health monitoring using micro-electromechanical sensors and systems (MEMS), J. Civ. Eng. Manage. 19 (1) (2013) S188-S201.
[24] R. Fedele, F.G. Praticò, G. Pellicano, Sustainable Road Infrastructures Using Smart Materials, NDT, and FEM-Based Crack Prediction, International Conference on Society with Future:Smart and Liveable Cities, Braga, Portugal, 318 (2020) 3–14.
[25] F.G. Praticò, R. Fedele, V. Naumov, T. Sauer, Detection and monitoring of bottom-up cracks in road pavement using a machine-learning approach, Algorithms 13 (4) (2020) 81. https://doi.org/10.3390/a13040081
[26] D.G. Goulias, S. Cafiso, A. Di Graziano, S.G. Saremi, V. Currao, Condition Assessment of Bridge Decks through Ground-Penetrating Radar in Bridge Management Systems, J. Perform. Constr. Facil. 34 (5) (2020) 1-13
[27] Standard Test Method for Determining the Thickness of Bound Pavement Layers Using Short-Pulse Radar. ASTM D4748-10. ASTM International, West Conshohocken, PA, USA, 2010.
[28] I. Al-Qadi, S. Lahouar, Part 4: Portland cement concrete pavement: measuring rebar cover depth in rigid pavements with ground-penetrating radar, Transp. Res. Rec. 1907 (2005) 80-85.
[29] Hexagon, K2_FW GPR system (IDS GeoRadar – Part of Hexagon, 2020), https://idsgeoradar.com/products.Accessed July 2020.
[30] S. Cafiso, A. Di Graziano, Monitoring and performance of AC pavements reinforced with steel mesh, Inter. J.Pavement Res. Technol. 2 (3) (2009) 82-90.
[31] R. Fedele, F.G. Praticò, Monitoring infrastructure asset through its acoustic signature, INTER-NOISE 2019 MADRID - 48th International Congress and Exhibition on Noise Control Engineering, Madrid, Spain, 2019.
[32] R. Fedele, F.G. Praticò, R. Carotenuto, F.G. Della Corte, Damage detection into road pavements through acoustic signature analysis: First results, 24th International Congress on Sound and Vibration, ICSV 2017, London, UK, 2017.
[33] M. Merenda, R. Carotenuto, F.G. Della Corte, F. G. Pratico, R. Fedele, Self-powered wireless IoT nodes for emergency management, Proc. 20th IEEE Mediterranean Electrotechnical Conference, MELECON 2020, Palermo, Italy, 2020.
[34] P.N. Schmalzer, Long-Term Pavement Performance Program Manual for Falling Weight Deflectometer Measurements. Report FHWA-HRT-06-132. Springfield, VA, USA, 2006 https://www.fhwa.dot.gov/publications/research/infrastructure/pavements/ltpp/06132/06132.pdf.
[35] Dyatest, ELMOD Software for Pavement Analysis. (Dynatest, 2020). www.dynatest.com. Accessed July 2020.
[36] R. Fedele, F.G. Praticò, G. Pellicano, The prediction of road cracks through acoustic signature: Extended finite element modeling and experiments, J. Test. Eval. 49 (4) (2019) https://doi.org/10.1520/JTE20190209
[37] E. Schubert, J. Wolfe, Timbral brightness and spectral centroid, Acta Acust. united with Acust. 92 (5) (2006) 820-825.
[38] J. M. Bland, D. G. Altman, Calculating correlation coefficients with repeated observations: part 1–correlation within subjects, BMJ 310 (6977) (1995) 446.
[39] J. M. Bland, D. G. Altman, Statistics notes: calculating correlation coefficients with repeated observations: part 2—correlation between subjects, BMJ 310 (6980) (1995) 633.
[40] K. Y. Liang, S. L. Zeger, Longitudinal data analysis using generalized linear models, Biometrika 73 (1) (1986) 13.
[41] D. McFadden, Conditional logit analysis of qualitative choice behavior. P. Zarembka (ed.), Frontiers in Econometrics. Academic Press, Cambridge, Massachusetts, USA, 1974, pp. 105-142.